A&A 569, A77 (2014)
DOI: 10.1051/0004-6361/201424099

Astronomy & Astrophysics

A laser-lock concept to reach cm s^{-1}-precision in Doppler experiments with Fabry-Pérot wavelength calibrators

A. Reiners[1], R. K. Banyal[1], and R. G. Ulbrich[2]

[1] Institut für Astrophysik, Friedrich-Hund-Platz 1, 37077 Göttingen, Germany
e-mail: Ansgar.Reiners@phys.uni-goettingen.de
[2] IV. Physikalisches Institut, Friedrich-Hund-Platz 1, 37077 Göttingen, Germany

Received 30 April 2014 / Accepted 6 August 2014

ABSTRACT

State-of-the-art Doppler experiments require wavelength calibration with precision at the cm s^{-1} level. A low-finesse Fabry-Pérot interferometer (FPI) can provide a wavelength comb with a very large bandwidth as required for astronomical experiments, but unavoidable spectral drifts are difficult to control. Instead of actively controlling the FPI cavity, we propose to passively stabilize the interferometer and track the time-dependent cavity length drift externally using the ^{87}Rb D_2 atomic line. A dual-finesse cavity allows drift tracking during observation. In the low-finesse spectral range, the cavity provides a comb transmission spectrum tailored to the astronomical spectrograph. The drift of the cavity length is monitored in the high-finesse range relative to an external standard: a single narrow transmission peak is locked to an external cavity diode laser and compared to an atomic frequency from a Doppler-free transition. Following standard locking schemes, tracking at sub-mm s^{-1} precision can be achieved. This is several orders of magnitude better than currently planned high-precision Doppler experiments, and it allows freedom for relaxed designs including the use of a single-finesse interferometer under certain conditions. All components for the proposed setup are readily available, rendering this approach particularly interesting for upcoming Doppler experiments. We also show that the large number of interference modes used in an astronomical FPI allows us to unambiguously identify the interference mode of each FPI transmission peak defining its absolute wavelength solution. The accuracy reached in each resonance with the laser concept is then defined by the cavity length that is determined from the one locked peak and by the group velocity dispersion. The latter can vary by several 100 m s^{-1} over the relevant frequency range and severely limits the accuracy of individual peak locations, although their interference modes are known. A potential way to determine the absolute peak positions is to externally measure the frequency of each individual peak with a laser frequency comb (LFC). Thus, the concept of laser-locked FPIs may be useful for applying the absolute accuracy of an LFC to astronomical spectrographs without the need for an LFC at the observatory.

Key words. techniques: radial velocities – instrumentation: spectrographs – planets and satellites: detection – techniques: spectroscopic

1. Introduction

High-precision radial velocity (RV) measurements have become a well established technique for detecting and characterizing planets around other stars, and they are in the focus for precision experiments like determing fundamental constants, measuring the cosmic microwave background temperature, and directly observating the expansion of the Universe (Maiolino et al. 2013). While the last experiments are among the main science cases for high-resolution spectroscopy at telescopes beyond the 10 m range, the search for exoplanets has become a focus of many observatories with telescopes on the 4 m scale. Instruments at these observatories require a cost-effective solution for high-precision wavelength calibration.

The gravitational pull exerted by an extrasolar planet causes reflex motion of the parent star detectable in the form of a small Doppler shift in the stellar spectra (e.g., Struve 1952; Marcy & Butler 1998; Mayor & Udry 2008). The major challenge for the RV method is to carry out high-precision measurements from tiny Doppler shifts of the host target over long periods of observations: an RV precision of ∼10 m s^{-1} can be sufficient to discover giant planets up to Jupiter or Neptune mass. Detection of low-mass planets like Earth requires measurements at a precision of 10 cm s^{-1} on timescales of years.

The key instrumental factors limiting the RV precision of spectrographic measurements are uncertainties in the wavelength calibration and instrument stability, particularly on timescales of years or decades. Additional uncertainties caused by the astronomical targets, like stellar activity jitter, are not considered here. Limiting factors include consequences from the insufficient stability of the instrument's line spread function owing to varying illumination (e.g., fiber scrambling, modal noise) and suboptimal knowledge about the wavelength solution. Traditional ways of calibrating the spectrograph rely on using fundamental atomic or molecular reference lines in optical and near infrared regions where astronomical spectroscopy is carried out. The most commonly used reference sources include Th- and U-based hollow cathode lamps (HCL), iodine or other gas absorption cells, and telluric lines in the Earth's atmosphere (e.g., Marcy & Butler 1992; Osterbrock et al. 1996; Kerber et al. 2007; Redman et al. 2012). Despite their simplicity, these calibration sources have certain drawbacks, such as uneven line spacing, a narrow spectral range, a large intensity difference between the bright and faint lines, and line blending and aging effects. All

these factors contribute to the final uncertainty in the wavelength solution (Pepe & Lovis 2008).

The perfect calibrator for astronomical RV experiments should provide a dense grid of evenly distributed spectral lines of uniform intensity in order to maximize the Doppler information content over the full wavelength range. Today, the ultimate solution for the wavelength calibration problem is expected to come from laser frequency combs (LFC) generated by femtosecond pulsed lasers (e.g., Murphy et al. 2007; Wilken et al. 2010; Steinmetz et al. 2008; Braje et al. 2008; Phillips et al. 2012). The self-referencing of the laser-comb lines produces exceptional stability and frequency precision (better than 10^{-15}) and is referenced to an atomic standard for very high accuracy. A drawback of most currently available systems is that the comb lines are very densely packed with frequency differences of only a few 100 MHz. The astronomical spectrographs used for RV experiments usually have a resolving power of 10–100 GHz, which is insufficient to resolve the narrowly spaced comb structure. To increase the comb line spacing, a common solution is to filter out most of the lines with external Fabry-Pérot (FP) cavities (Steinmetz et al. 2009; Braje et al. 2008; Quinlan et al. 2010). The filtering process itself requires very high accuracy and can induce noise in the piezoelectrically controlled cavities. Therefore, exactly fine-tuning the single-finesse cavity's free spectral range (FSR) to the desired repetition frequency of the comb lines is demanding. Other technical challenges include the broadband coating dispersion of the cavity mirror, causing some mismatch between the comb lines and the cavity resonance and imperfect filtering arising from a relatively broad cavity linewidth. The light leakage from the partly attenuated modes gets amplified in the final stage of the second harmonic generation, thus shifting the line center observed by the spectrograph (Schmidt et al. 2008). Such technical difficulties are likely to be overcome during the next years, but the question when LFC technology becomes a turn-key and affordable solution for astronomical observatories is still open.

A simple and elegant approach to generating a "perfect" reference spectrum is to use the cavity resonance lines of a Fabry-Pérot interferometer (FPI) illuminated with white light (and without stabilizing it with an LFC; Wildi et al. 2009, 2010; Halverson et al. 2012). A passively stabilized "ideal" FPI that is illuminated with a broadband light source produces transmission lines that are equidistant in frequency space. The position, linewidth, spacing, and amplitude of these synthetic lines can be easily tailored to match the spectrograph requirements. The challenge for the passive FPI is that frequency drifts can occur for many reasons, including changing environmental conditions, and that active control of an FPI tailored for astronomical research is very difficult at m s^{-1} accuracy. A simple solution for astronomical programs is to cross-check the calibration spectrum of the FPI against classical calibration methods like HCLs, which can be done during daytime. This strategy, however, is again limited by the accuracy of the HCLs (and their practical problems).

Our solution is to passively stabilize the FPI and track the drift on an absolute scale, for example, relative to an atomic transition. To reach the high precision and long-term stability of the FPI cavity, we propose a laser-lock concept to track the dimensional stability of a dual-finesse FPI cavity using frequency stabilized diode lasers. The mechanism exploits the high accuracy of optical frequency measurements and connects it to wavelength standards useful in astronomy. Our strategy eliminates the need for comparing the FPI signal to gas emission lines on the CCD and provides absolute calibration during observation.

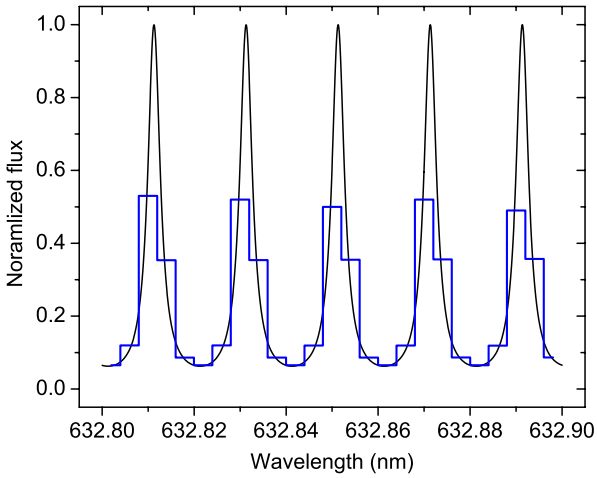

Fig. 1. FPI interference pattern (black, $\mathcal{F} = 10$) sampled by the astronomical spectrograph (blue) with a resolving power of $R = 80\,000$.

Such a system has all advantages of the optical frequency comb but can be built entirely from simpler (and cheaper) off-the-shelf technology. In this paper, we introduce a concept that utilizes frequency metrology techniques to track the stability of FP calibrators for astronomical use. The level of implementation details is kept to a minimum in order to introduce the concept clearly and to avoid confusion between technical shortcomings and general limitations, the latter being the main obstacle in current solutions for astronomical wavelength calibration.

In Sect. 2, we discuss instrument stability and design requirements. The laser-lock concept and the dual-channel FPI are described in Sects. 3 and 4, respectively. A discussion of laser frequency control relevant to laser-locking is provided in Sect. 5. A method for establishing an absolute frequency scale for FPI calibration is proposed in Sect. 6. Finally, we present a summary in Sect. 6.

2. The FPI transmission spectrum

To reach the level of thermal and mechanical stability required for sub-m s^{-1} accuracy is a challenging task in astronomical Doppler experiments. In an echelle spectrograph, frequency calibration must be provided by a spectral standard recorded on the very same detector as the one optimized for astronomical observations. Therefore, spectral resolving power and light intensity cannot be chosen arbitrarily. For the purpose of frequency calibration in astronomy, FPIs have several advantages over other calibration sources, their main disadvantage being that they do not inherently provide an absolute frequency standard.

When illuminated with a white light source the gain-free FPI produces a series of discrete cavity resonance lines separated by a fixed frequency $\Delta\nu_{\rm FSR} = c/(2nl)$, where n is the refractive index of the cavity medium and l the length. A model spectrum of an FPI is shown in Fig. 1. The main specifications for an optimal FPI frequency calibration spectrum are defined by the characteristics of astronomical spectrographs, which are the following:

– The FPI lines should span the full wavelength range of the spectrograph and allow as much light as possible to enter the spectrograph. This entails the need for high-reflectance broadband coated cavity mirrors and a trade-off between peak width and the amount of light available for calibration. These requirements limit the reflectivity to roughly $R \simeq 70\%$, resulting in rather low values for the finesse $\mathcal{F} = \pi R^{1/2}/(1-R) \lesssim 10$.

- The full width at half maximum (FWHM) of the transmission peaks should be close to (or below) the spectral resolving power of the instrument. The FWHM is determined by the finesse $\mathcal{F}$ of the interferometer through $FWHM = \mathrm{FSR}/\mathcal{F}$, i.e., the FSR divided by the finesse. With the numbers used above, a typical FWHM of such an FPI is smaller than the spectrograph resolution, but is still several hundred m s^{-1} to one km s^{-1}.
- For optimal sampling, the FSR, i.e., the spacing between individual lines should be on the order of $3 \times FWHM$ of the spectrograph resolution. This is a compromise between spectral resolving power, transmission peak contrast, and maximizing the gradient of the signal over a wide spectral range. Wider spacing results in imperfect sampling (spectral regions with no frequency information), while too narrowly spaced lines cannot be resolved and lead to diminished contrast.

In general, the total line-position error σ_ν from photon noise in an FPI transmission spectrum with N comb lines, whose FWHM is sampled by p pixels each, can be approximated by (Brault 1987)

$$\sigma_\nu = \frac{A}{\sqrt{Np}} \frac{FWHM}{S/N}. \quad (1)$$

Here, S/N is the peak signal-to-noise ratio and A (<1) a normalization constant that depends on the shape of the line profile. According to Eq. (1), a spectrum of an FPI with $N \approx 10^4$ lines, $p = 10$, $S/N = 100$, and a FWHM of 1.5 GHz (15 GHz FSR and $\mathcal{F} = 10$) would reduce the total frequency offset uncertainty to approximately 3 cm s^{-1} at $\lambda = 600$ nm and 6 cm s^{-1} at $\lambda = 1200$ nm. This performance is easily achieved in currently existing spectrographs and meets the required precision of almost all astronomical RV measurement carried out today. It shows that FPI spectra in general are well suited to the frequency calibration of astronomical RV experiments.

The operational success of the FPI method depends crucially on the dimensional stability of the cavity. Any perturbations in FPI cavity length L or refractive index n would contribute as a shift in the transmission peaks. For example, to achieve an RV precision of 10 cm s^{-1} with an FPI that has a FSR of 15 GHz, the cavity length must be stable to roughly 10^{-10} cm. For low-expansion material (thermal expansion coefficient $\alpha \sim 10^{-8}$ K^{-1}), this translates to a temperature stability of a few mK (Schäfer & Reiners 2012). To further minimize the effect of a varying refractive index n on the optical path length, the FPI must be placed inside a mechanically and thermally stable evacuated chamber. Residual drifts in cavity length can be estimated indirectly from rms temperature fluctuations measured inside the vacuum chamber. Such measurements also have errors arising from a) the uncertainties associated with the thermal expansion coefficients and b) the placement of the temperature sensors away from the optical path of the cavity.

A fundamental requirement for long-term stability is that the dispersion of the cavity is constant with time. The change in mirror dispersion can result from wavelength-dependent instabilities of the optical path or from changes in the optical properties of the coating. The former is minimized by avoiding any color-dependent optical elements. For the latter, mechanical stress (specific to coating process), aging, and light-induced damage (mostly from high power lasers) are known to alter the reflectance of the mirror over time (Ennos 1966; de Denus-Baillargeon et al. 2014). With an FP housed in a thermally controlled evacuated chamber, we believe dispersion variations would not be a major concern within a few years of operation, but experimental prove of this assumption is not available yet. All together, it is an extremely challenging problem to design an FPI that can fulfill the stability requirements for cm s^{-1} accuracy over several years, which are the typical timescales for astronomical experiments. A solution to this problem is to accept that the FPI will not be stable at the required level of precision and to accurately determine the amount of the drift, i.e., to track the variation of the mirror distance (but still assuming that the dispersion is constant). We propose to solve this problem by exploiting the metrology precision available from optical frequency standards.

3. The laser-lock concept

The requirements that FPI stability reaches cm s^{-1} long-term accuracy by a long way exceeds today's technological possibilities. An alternative to perfect stability is to accurately track this drift. A straightforward way of implementing this is to cross-calibrate the FPI spectrum with the primary wavelength standards used in astronomy, for example HCL or gas absorption cells. This can be done using the astronomical spectrograph, and this strategy could improve most of today's standard wavelength calibration procedures. The main improvements are the clean FPI spectrum useful for continuous drift check measurements and interpolation of the standard wavelength solution in areas where primary standards have no spectral features. This strategy, however, is fairly indirect and causes a large overhead in calibration exposures, and it relies on the use of other primary standards with all their shortcomings and measured in the astronomical spectrograph. More direct drift-tracking of the FPI transmission spectrum without involving the astronomical spectrograph would be highly desirable.

Spectroscopic measurements based on spatial interference (at the grating) measure wavelengths rather than frequencies of the electromagnetic waves. The resolution of dispersion-based instruments invariably suffers from unavoidable wavefront aberrations in the optical system and from the vast difference between the accuracy desired (fractions of wavelengths) and the physical dimensions of optical components. Frequency-measuring techniques, on the other hand, have resulted in accuracies that are several orders of magnitude higher than any wavelength measurement carried out with spectrographs or interferometers (e.g., Udem et al. 2002). Advances in laser metrology allow us to connect the precision of frequency standards to other physical quantities, including the measurement of the dimensional stability of instruments (Riehle 1998). It is this advantage that is utilized to reach accuracies achieved, for example, by the laser-comb technology.

Employing the advantage of frequency standards, we intend to use an optical heterodyning technique to directly measure the FPI cavity drift. We propose to track the center position of one FPI resonance peak by comparing it to a standard frequency provided by an external standard, such as the ^{87}Rb D_2 line. The proposed setup is shown in Fig. 2. Light from the telescope is fed into the astronomical spectrograph together with the light comb from the FPI (upper part of Fig. 2). The two frequencies of one FPI resonance peak and the frequency standard (Rb cell) are locked to a frequency stabilized external cavity diode laser (ECDL) operating at 780 nm; at ECDL-1, the laser is locked to the cavity after being shifted by an electro-optical modulator, at ECDL-2 it is locked to Doppler-free hyper-transitions of the Rb atom.

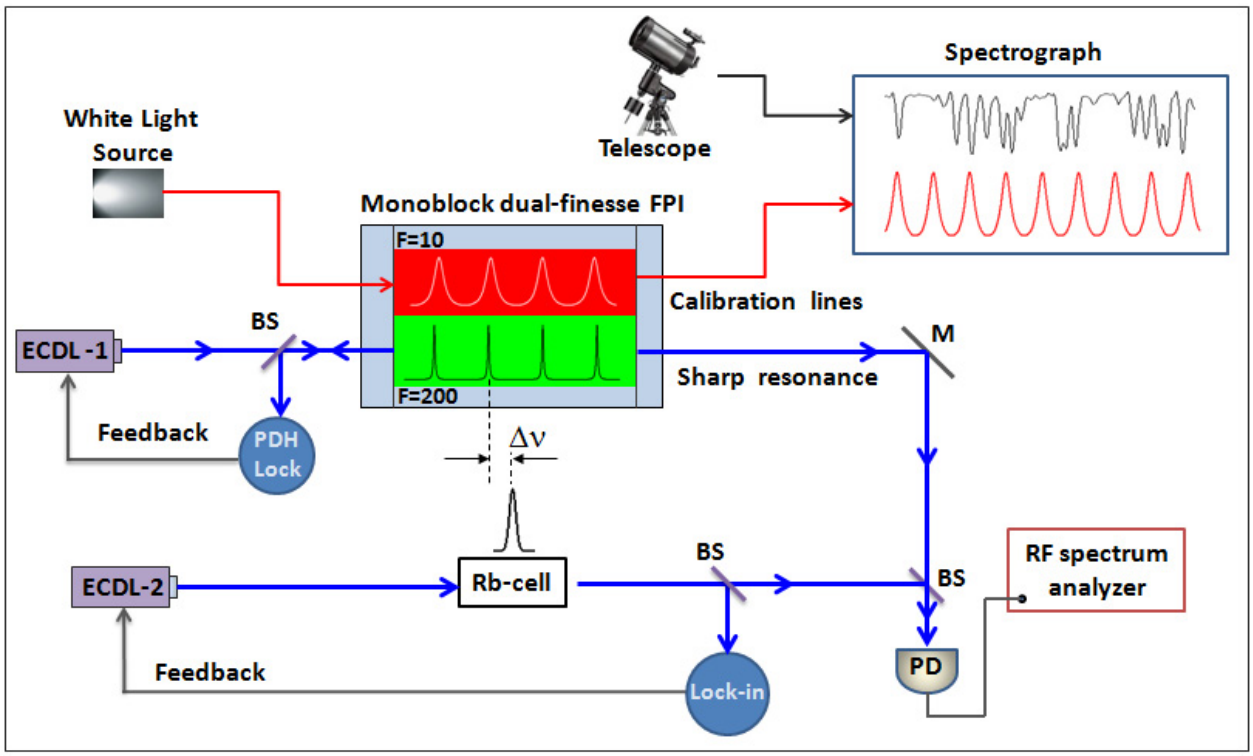

Fig. 2. Scheme of the proposed laser-lock system for tracking the FPI cavity. A white light continuum source illuminates the low-finesse Channel-1 interferometer (red block) to produce calibration lines for an Echelle spectrograph. The high-finesse Channel-2 (green block) provides an external reference for locking the frequency of the diode laser ECDL-1 to the FPI cavity. The RF-beat signal produced from interference between the Rb-locked ECDL-2 and the cavity locked ECDL-1 is recorded by high-speed photodetector PD. The cavity drift is to be inferred from the change in beat frequency.

The locking mechanism ensures that any systematic or random drift in cavity length is transferred to the frequency change in the ECDL-1, and it accurately ties the frequency of ECDL-2 to a well-defined physical standard. The beat between the two laser frequencies is then measured at the photodetector (PD). The temporal interference between two overlapping coherent fields with slightly different optical frequencies ($\nu_{1,2} \sim 10^{14}$ Hz) from ECDL-1 and ECDL-2 creates a radio-frequency (RF) beat signal at much lower frequency ($\Delta f = |\nu_1 - \nu_2| \approx 10^6$–$10^9$ Hz). The amplitude and phase of the beat signal is easily measured with a high speed PD. The output of the PD is processed electronically by an RF spectrum analyzer or a digital frequency counter. Since the atomic transitions are largely insensitive to external factors, the frequency of ECDL-2, once locked to the Rb-cell, remains stable. Any change in the beat signal would result from a frequency shift in ECDL-1 following the FPI cavity drift.

The proposed concept foresees tracking of the FPI, which in principle does not require very high stability. Nevertheless, in practice, passive stabilization of the FPI (temperature and pressure) is needed to ensure that the cavity does not drift more than a mode-hop free scanning range of the diode laser, which is typically 5–6 GHz. Beyond this range, the laser frequency could suddenly jump to random values, breaking the lock with the consequence of losing the tracking. A larger cavity drift would also create an ambiguity in keeping the cavity tied to Rb-line within 1/2 FSR. It is technically possible to increase the mode-hop free tuning range of the laser (e.g., by using current feed-forward), but a freely drifting cavity at ambient temperature and pressure would place unrealistic demands on the speed and bandwidth of photodetector system, thus increasing the complexity and overall cost beyond any practical limits.

4. The Dual-finesse FPI cavity

A dual-finesse FPI cavity is similar to regular FPI, but it has a coating with wavelength-dependent reflectivity. For example, a reflectivity of 99% can be reached around 780 nm, the wavelength range useful for standard Rb cells, and falls off to 70% over wide wavelength ranges. This cavity has low finesse ($\mathcal{F} \approx 10$) everywhere but around 780 nm where its transmission peaks will be very sharp ($\mathcal{F} = 200$). As noted earlier, the high-finesse mirrors usually have narrow wavelength ranges and are therefore not suitable for astronomical use where the entire spectral range should be calibrated. On the other hand, the accuracy with which the laser beam can be locked to the FPI cavity is a function of the transmission peaks' FWHM. This accuracy is substantially lower than the overall zero-point precision of the FPI because the laser beam is locked to one single peak alone but not to the entire comb ($N = 1$ in Eq. (1)). An FPI with a frequency-selective finesse is a useful combination of coverage and precision. It has the great advantage that the light used for RV calibration and the light for frequency locking follows an identical optical path that eliminates uncertainties possibly introduced by solutions using physically different surfaces.

Figure 3 shows a comparison between a resonance line from a $\mathcal{F} = 10$ FPI and a $\mathcal{F} = 200$ FPI. The position of the second line can be measured at substantially higher accuracy, which can be seen from Eq. (1): $N = 1$ (i.e., only one transmission peak is used), the transmission peak S/N is approximately the same for different values of the cavity finesse, $\mathcal{F}$, the number of pixels sampled per FWHM, p, and FWHM scale with FWHM, i.e., $\sigma_\nu \propto \sqrt{FWHM}$. As an example, we assume that the locking is carried out at roughly $S/N \approx 1000$. For an FPI with

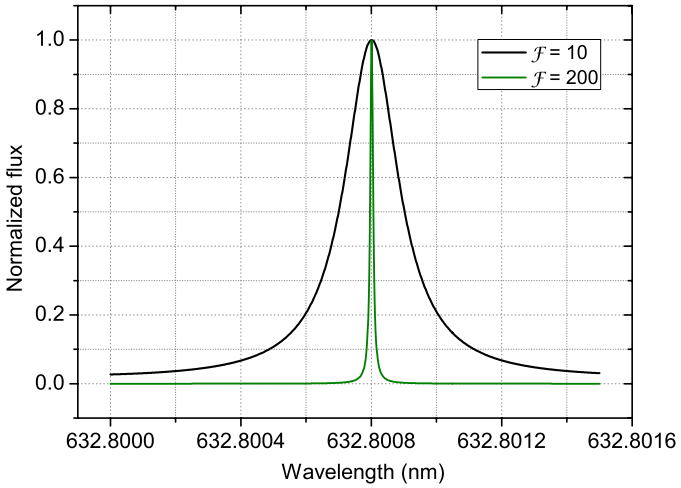

Fig. 3. Comparison between a broad line (black curve, $\mathcal{F}$ = 10) from a low-finesse FPI and a narrow line (green curve, $\mathcal{F}$ = 200) from a high-finesse FPI.

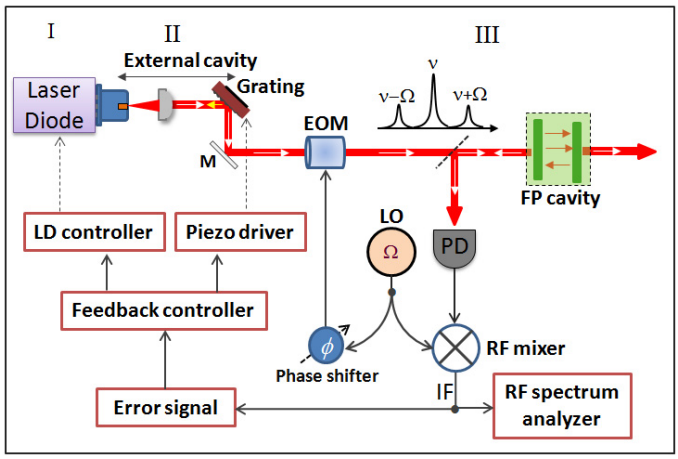

Fig. 4. Frequency stabilization of a semiconductor diode laser with the Pound-Drever-Hall technique (see, e.g., Drever et al. 1983). In Stage I, the linewidth of the laser is passively stabilized to ~10 MHz level by keeping the temperature and diode current stable. The grating feedback in Stage II reduces the linewidth to a few MHz. In Stage III, an active feedback mechanism reduces the linewidth further to about 100 kHz range by locking the laser frequency to the FPI cavity or the Rb-cell. Some other components, e.g., Faraday isolator and polarization optics, are not shown in the layout. LD: laser diode; EOM: electro-optic modulator; RF: radio frequency; PD: photodetector; LO: local oscillator.

FSR = 15 GHz this results in a precision of roughly 1.5 cm s^{-1} for a $\mathcal{F}$ = 200 FPI (*FWHM* = 75 MHz) and 30 cm s^{-1} for a $\mathcal{F}$ = 10 FPI (*FWHM* = 1.5 GHz) at 600 nm. The same accuracy is reached using an FPI with an FSR of 7.5 GHz operated at 1200 nm. The best S/N can be achieved with a high *spectral power density* source. A single-line laser diode with 30 mW output is sufficient to reach this high S/N within a relatively short time (~minutes).

In our dual-finesse cavity, the FSR and linewidth in the low-finesse range comb lines are optimized for use in astronomical spectra. The second part has an FSR set by this choice of parameters, but its finesse is higher, so the FWHM is smaller to allow a more precise determination of the transmission peak frequency.

For the success of the locking concept, it is crucial that the light entering the FPI follows a well-defined and stable optical path. This is best achieved with single-mode fibers (SMF), and for the FP calibrator, the choice of SMFs probably is absolute necessity. For effective mode matching, the laser beam and white light source must couple completely into the fundamental spatial mode of the cavity (Anderson 1984). Any departure from this condition may produce undesirable artifacts in the calibration lines and render the laser locking scheme ineffective. The calibration lines, e.g., produced in an FP cavity illuminated with multimode fiber (core diameter >10 μm) can be highly asymmetric (Schäfer & Reiners, in prep.). This asymmetry is caused by small angular and/or transverse offset between the fiber axis and the cavity axis and it is found to increase with the fiber core diameter, producing RV errors in excess of several 100 m s^{-1}. For astronomical use (telescope → spectrograph in Fig. 2), SMFs are avoided mainly because of the light losses and difficulty coupling light efficiently in SMFs, but this limitation does not apply to our FPI scheme, at least not until the white light leaves the FPI on its way into the astronomical spectrograph. The necessity of SMFs for the white light path requires high intensity of the light source, for example from a white laser.

5. Laser frequency control

In the proposed setup shown in Fig. 2, two single frequency laser beams are required to track the FPI cavity drift. A frequency stabilized ECDL can be constructed using off-the-shelf components (e.g., Ricci et al. 1995; Arnold et al. 1998). A generic frequency stabilization scheme for an ECDL is shown in Fig. 4. Prior to frequency locking, it is necessary to enhance the passive stability of the diode to realize single-mode operation.

5.1. Passive frequency stabilization

The frequency of the laser diode is primarily determined by the gain profile and longitudinal cavity modes that are normally separated by 100–200 GHz. A typical index-guided laser diode operates at a cavity mode that experiences the maximum gain. The laser frequency randomly jumps from one mode to another owing to variations in cavity length and the gain profile caused by random fluctuations in temperature and injection current (phase noise). The frequency shift with temperature and current is on the order of 100 MHz/mK and ~3 MHz/μA, respectively (Saliba et al. 2009). By stabilizing the diode temperature to a mK level and reducing the rms injection current noise to ≤1 μA, a single-frequency, mode-hop-free operation (Stage I in Fig. 4) can be realized.

The phase-noise limit (also called Schawlow-Townes linewidth) of the laser is proportional to the inverse square of the cavity length (Henry 1986; Osinski & Buus 1987). Therefore, the next step to minimize the phase noise limit is to increase the cavity length L of the laser. This is achieved by adding an external reflector to the laser diode. Stage II in Fig. 4 shows the diffraction grating used in Littrow configuration to form an extended cavity with the rear facet of the diode. Many other variants of external cavities can be found in the literature (e.g., Mroziewicz 2008). The extended cavity effectively reduces the phase noise, and the wavelength-selective feedback from the grating narrows the laser linewidth further to a few 100 kHz. A continuous wavelength scan up to several GHz is easily achieved by tuning the grating angle or changing the resonator length.

The linewidth of the ECDL is significantly narrower than the solitary diode laser. However, owing to extreme temperature sensitivities and reduced mode spacings, the laser output becomes highly prone to mode-hopping. The laser itself is therefore not

sufficient as absolute wavelength standard, and further stability of the laser frequency can only be ensured by actively locking the laser to a fixed frequency reference.

5.2. Active frequency stabilization

To measure the FPI drift below 10 cm s^{-1} and to monitor the long-term stability of the cavity, the laser frequency spread should be reduced to a few 100 kHz or below. A stable linewidth close to 100 kHz can be achieved by locking the laser to an external reference frequency. Deviations from the reference frequency are measured in real time and corrected with an appropriate feedback. An active stabilization requires fast electronic feedback control and a frequency discriminator for suppressing the drifts and high frequency technical noise caused by acoustics and mechanical vibrations (Fox et al. 2003).

Fundamentally, all locking methods rely on generating an *error signal* that is proportional to the frequency deviations of the laser source from the fixed reference. A steep slope about the lock point result in a larger error and improved noise sensitivity. Various modulation techniques are used for generating the error signal (Neuhaus 2009). The choice of modulation frequency depends on the characteristic linewidth of the spectral signal obtained from the reference source (Bjorklund 1980). For example, to lock the laser to the Doppler-free Rb line (typical $FWHM \sim 6-8$ MHz), low modulation frequencies of the diode current up to a few 100 kHz are preferred. Keeping the modulation frequency within the range of a few 100 kHz is necessary to prevent sideband interference with many closely spaced hyperfine and crossover transitions in the atomic lines.

A very effective and high frequency modulation can be employed in a Pound-Drever-Hall locking technique, represented as Stage III in Fig. 4. PDH is a method for frequency stabilization (Drever et al. 1983) that produces a robust lock that is immune to intrinsic fluctuations in laser power. It has a wide frequency-capture range and is capable of suppressing high-frequency technical noise well beyond the cavity response time. A detailed quantitative description of the PDH technique is given by Black (2001). Here, we give a brief summary of the technique along with the key requirements relevant to our needs.

- The PDH lock operates on a light beam reflected from the FPI cavity. A monochromatic light beam whose frequency is an integral multiple of the cavity-FSR is completely transmitted, while an off-resonance beam is completely reflected. The reflected beam experiences a definitive phase shift that depends on its frequency with respect to the cavity resonance. The intensity of a reflected beam from an FPI cavity is plotted, together with its phase in Fig. 5 (upper panel). The phase of the reflected beam, shown only for the carrier frequency in Fig. 5, has a sharp transition in the vicinity of the cavity resonance, which is used as a high-fidelity frequency discriminant to generate an error signal. For frequencies significantly *above* and *below* the cavity resonance, the phase shift, respectively, approaches a fixed value of +180° and −180°.
- To generate the error signal, the carrier frequency ν of the laser first is phase-modulated by a Pockels cell driven by a RF oscillator. The phase modulation of the laser beam creates two frequency sidebands at $\nu \pm \Omega$. To ensure an extended lock range beyond the cavity linewidth, the modulation frequency Ω must be a few times the FWHM of the cavity but should not exceed its FSR. For example, for a cavity with FSR = 15 GHz and $FWHM$ = 75 MHz, sidebands at $\Omega \sim \pm 500$ MHz would effectively overcome any technical noise in the laser frequency.
- When a frequency-modulated beam is incident on the cavity, the two sidebands (that are outside the cavity resonance) are completely reflected with a +180° phase shift (the $\nu+\Omega$ component) and −180° (the $\nu-\Omega$ component). The carrier is also partly reflected if its frequency ν is slightly off resonance. Superposition of the reflected carrier and the sidebands generates a beat signal with $\sin \Omega t$ and $\cos 2\Omega t$ terms at the photodetector (see Black 2001, for an exact derivation). The Ω term represents the interference between carrier and sidebands, while the 2Ω term results from interference between the two sidebands. The amplitude and the sign of the Ω term is extracted by RF-mixing of the photodetector output with the local oscillator signal (see Fig. 4). The sign of the extracted signal determines which side of the resonance the laser frequency has drifted, while the amplitude provides the error signal proportional to the frequency deviation. A typical error signal is shown in the lower panel of Fig. 5 for the laser frequency excursions in units of cavity FSR.
- The task of the feedback system is to use this error signal for adjusting the laser frequency by controlling one or more tuning parameters (injection current, temperature, or piezo-controlled cavity length) of the laser. In practice, a high servo gain and large bandwidth of the frequency tuning elements are needed to suppress the laser's intrinsic noise (Fox et al. 2003).

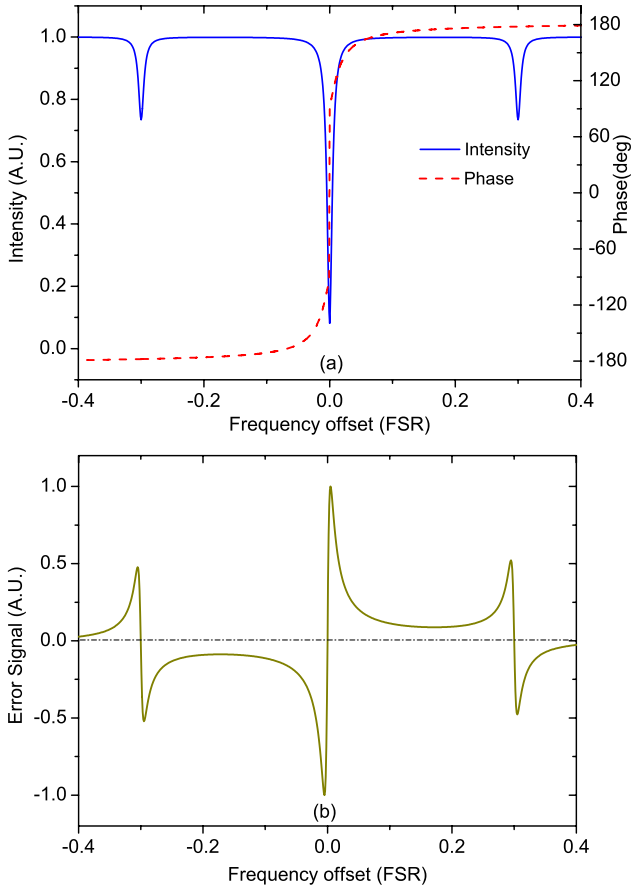

Fig. 5. a) Intensity (blue curve) and phase shift (red curve) of a reflected carrier from an optical cavity with $\mathcal{F} = 200$. **b)** The expected PDH error signal (the $\sin \Omega t$-term, see text) with sidebands located within 30% of the FSR. Laser is locked to the zero-crossing point of the error signal where the slope is steepest.

5.3. Noise and performance limitations

The accuracy of cavity drift measurements from the optical-beat signal depends on the noise in the error signal. At optimum locking condition (highest S/N), the shot-noise limit determines the intrinsic frequency fluctuations of the laser. These fluctuations cannot be distinguished from actual frequency changes caused by the cavity drift. Laser frequency uncertainty associated with shot noise can be expressed as (Drever et al. 1983)

$$\delta\nu(\tau) \geq FWHM \left(\frac{hc}{P_0 T \eta \lambda}\right)^{1/2} \left(\frac{1}{\tau}\right)^{1/2}, \quad (2)$$

where FWHM is the cavity width, P_0 the laser power, T is the cavity transmission efficiency, η the quantum efficiency of the photodetector, and $(2\pi\tau)^{-1}$ the observation bandwidth. For an FPI cavity of $FWHM = 100$ MHz, laser power $P_0 = 1$ mW, $\lambda = 780$ nm, $\eta = 0.9$, $T = 0.2$, and $(2\pi\tau)^{-1} = 1$ kHz, we calculate $\delta\nu(\tau) \approx 300$ Hz as the frequency stability limit from Eq. (2). This corresponds to a precision of $\delta L/L = \delta\nu/\nu \approx 7.8 \times 10^{-13}$; $v \approx 0.2$ mm s^{-1}. This shows that our proposed locking scheme can determine the position of the FPI transmission peaks with a precision that is safely beyond the calibration requirements for all relevant Doppler experiments planned for the near future.

The fundamental anchor of the calibration scheme is the stability of the Rb atom. We are not aware of any specific evaluation of the stability of a Rb cell over an extended period of time. Some attempts have been made to identify and evaluate the impact of various parameters and experimental conditions that can influence the long-term, $>10^5$ s, and short-term stability of Rb standards (Ye et al. 1996; Vanier & Mandache 2007; Affolderbach et al. 2004). The most notable factors that can perturb the sub-Doppler lines of Rb atoms are fluctuations in the cell temperature and a surrounding magnetic field. Minimizing these sources of noise is not a fundamental problem. The magnetic sub-level shifting/splittings are a few MHz/G (Steck 2010), and they can be largely eliminated by enclosing the Rb-cell inside a field-proof casing capable of attenuating the effect of external magnetic field to the level of a few μG. Furthermore, the hyperfine levels of the ^{87}Rb isotope are less susceptible to magnetic interference than ^{85}Rb. This advantage comes from the smaller nuclear spin ($I = 3/2$) of ^{87}Rb resulting in fewer Zeeman sublevels as compared to ^{85}Rb85 ($I = 5/2$). Finally, requirements on the thermal control of the Rb cell are moderate because the temperature coefficient for line shifts is about 10^{-11}/K (Affolderbach et al. 2004). A modest thermal stability of ~100 mK of the cell is sufficient to keep the temperature-dependent drifts at least one order of magnitude below the required RV precision.

6. From precision to accuracy

The locking scheme introduced above tracks variations of the FPI spacer length precisely so that its uncontrolled drift can be corrected on a cm s^{-1} level. To compare measurements from different instruments and to provide an absolute wavelength scale for the astronomical measurements, it would be desirable to know the *absolute* frequency of the FPI transmission peaks. For this, we need to identify the order of interference, m, of the peaks, which is analogous to accurately determining the length of the spacer. In this section, we investigate the question of whether an absolute frequency scale can be established from an FPI spectrum in an astronomical spectrograph (see Meissner 1941; Born & Wolf 1999). The derivation of an absolute frequency scale also works without the locking part but with reduced precision.

The transmittance, T, of an FPI can be described by *Airy's* formula,

$$T = \frac{1}{1 + F \sin^2 \delta/2}, \quad (3)$$

with $F = 4\mathcal{R}/(1-\mathcal{R}^2)$ and $\mathcal{R}$ the reflectivity. The phase, δ, determines the positions of the maxima according to the conditions of interference:

$$\delta_m = \frac{4\pi}{\lambda_m} nl \cos\theta = 2\pi m, \quad (4)$$

with λ_m the wavelength, n the index of refraction, l the length of the spacer, and θ the angle between the incoming light and the interferometer surface. In the special case of $n = 1$ and perpendicular illumination ($\cos\theta = 1$), the condition for the transmission peaks simplifies to

$$\lambda_m = 2\frac{l}{m}. \quad (5)$$

The transmission peaks of an FPI are equidistant in frequency space (ν), and the spacing is

$$\Delta\nu = \mathrm{FSR} = \frac{c}{2l}, \quad (6)$$

with c the speed of light. Equation (6) shows the immediate correspondence between spacer length l and the peak spacing, $\Delta\nu = \mathrm{FSR}$. This means that if we can accurately measure the distance between the transmission peaks, we can calculate l and find the absolute wavelength solution for our FPI spectrum.

We can uniquely identify the order number m of a transmission peak in the FPI spectrum if we can estimate λ_m from Eq. (5) with an uncertainty $\delta\lambda_m$ that is smaller than the distance between two peaks (FSR). We show in the following that for this exercise, it is not necessary to determine the position of two transmission peaks (defining FSR) through ultra-high precision measurements, but that the accuracy provided with standard calibration techniques in the astronomical spectrograph is sufficient. An approximate wavelength scale can, for example, be established from a HCL or a pen ray lamp in order to define the position of at least two FPI transmission peaks. An accuracy on the order of 100 m s^{-1} (~150 MHz) is easily achieved for the individual lines. The uncertainty in the difference between the two peaks is then approximately $\delta\nu = 210$ MHz. In relation to the FSR, this translates into an unacceptable uncertainty of $\delta\lambda_m = 4000$ km s^{-1} for the absolute peak positions. However, the large lever arm of $\Delta m \sim 10^4$ transmission peaks observed in an FPI spectrum tailored for astronomical experiments solves this problem, because we can select one transmission peak at the blue end of the spectrum and a second at the red end, measure their positions, and count the number of transmission peaks, Δm, between them (method of exact fractions). The relative uncertainty δl in the measurement of the FPI spacing, l, can now be derived with the significantly reduced relative uncertainty of

$$\frac{\delta l}{l} = \frac{\delta\mathrm{FSR}}{\mathrm{FSR}} \frac{1}{\Delta m}. \quad (7)$$

This is approximately 1.3×10^{-6} for the numbers above, which means an uncertainty in the *absolute* frequency of $\delta\lambda_m \approx 400$ m s^{-1}. This is much lower than the approximate 9 km s^{-1} spacing of FPI peaks. We can therefore uniquely identify the mode of interference, m, for *all* transmission peaks if we know the exact position of one single peak (using a locking scheme)

Table 1. Summary of typical parameters for FPI frequency calibration; for the FPI we assume FSR = 15 GHz, $\lambda = 600$ nm.

Type of operation	$\mathcal{F}$	N	S/N	δv
"Astro"	10	10 000	100	2.8 cm s^{-1}
single-peak "Astro"	10	1	1000	28.5 cm s^{-1}
single-peak high-$\mathcal{F}$	200	1	1000	1.4 cm s^{-1}

and can obtain a wavelength solution with relaxed accuracy for the rest of the wavelength range.

The identification of m, however, does not accurately define the absolute wavelength of all peaks. Although our locking scheme provides l for the wavelength used for the locking scheme, we cannot assume that l is identical for all other wavelengths. The problem is that the coating of our FPI has a very substantial extension relative to l and that phase changes can become important in interferometers with dielectric coatings (e.g., Stanley & Andrew 1964; Bennett 1964; Lichten 1985, 1986). In other words, δl is not well known for all peaks because the penetration depth of the light into the coating (or the group velocity dispersion) is unknown. The thickness of a coating is typically a few μm, which means that the uncertainty in l, hence the absolute uncertainty of a transmission peak, is up to $d/l \approx 10^{-6}/10^{-2} = 10^{-4}$ (but its effect on the FSR may be reduced using chirped systems, Szipöcs et al. 1994). The absolute uncertainty of individual transmission peaks can therefore be as large as many km s^{-1}. On the other hand, the penetration depth varies smoothly as a function of frequency, which means that the FSR varies slowly, and the distance between individual peaks varies slowly, too, which can help construct the absolute wavelength scale. Nevertheless, the wavelength dependence of FPI thickness and phase change upon reflection are serious problems if FPIs are to be used for absolute wavelength calibration, and the problem is even greater if the etalon has smaller spacing (for example, fiber etalons). This problem has been discussed thoroughly in the literature and finally led to the development of the LFC in which every single comb peak is accurately defined.

7. Summary

A Fabry-Pérot interferometer operated with a white light lamp can provide a large number of well-defined and uniform transmission peaks that are suitable for frequency calibration in astronomical spectrographs. We discussed advantages and challenges of FPI frequency calibration and a laser-lock concept to precisely track frequency offsets. A summary of the possible operation modes and precisions reached in the measurement of frequency offsets is given in Table 1.

The high number of available lines from an FPI tailored to astronomical research can provide cm s^{-1} precision if the FPI is operated at a peak S/N around 100, which is a realistic value for simultaneous wavelength calibration. The problem with such an FPI is that stabilization of the cavity length to this level of precision is impractical so that the cavity drift contributes a larger uncertainty than the actual determination of the transmission peak position in the astronomical spectrograph.

The solution we proposed is to track the cavity drift by comparing the position of one transmission peak to an external standard, e.g., an atomic Rb transition. The measurement of a single line peak position in the same FPI that is used for the astronomical measurement cannot be measured with m s^{-1} precision at a S/N of 100, and the same is true for any other spectral feature from external sources in the spectrograph itself. This measurement has to be carried out externally where it can be done at much higher S/N. For example, at $S/N = 1000$ the uncertainty in the peak position is roughly 30 cm s^{-1}, which may already be useful for astronomical purposes. An extension to this concept is to use a second FPI with higher finesse; our proposal foresees a dual-finesse cavity with an optimized reflectivity that varies with wavelength. With a finesse of 200 and a S/N of 1000 a simple tracking mechanism can track the offset at a precision of roughly 1 cm s^{-1} using a single line in a wavelength region where the cavity has high reflectivity. A notch filter can be used to prevent the high intensity of the laser from entering the spectrograph. Another improvement is the implementation of a locking mechanism, such as PDH. This ensures a measurement precision of the drift between the FPI and the external standard that is only a fraction of a mm s^{-1}.

Several other solutions that track the drift of the interferometer are possible. For example, as a compromise between rather low finesse for the broad (astronomical) range and relatively high finesse for tracking, one may choose $\mathcal{F} \approx 50$ for the entire wavelength range. Such an FPI can cover a wide wavelength range and still provide relatively high single-line precision when measured at high S/N. With a typical exposure time of several minutes, integration times for the drift tracking are long enough to measure the drift at much higher S/N than 1000, which relaxes the requirements for all other parameters.

The wide wavelength range of an astronomical FPI also allows the mode of interference to be determined for all transmission peaks. This is possible when two transmission peaks can be measured that are separated by a large difference in interference mode number; the relative uncertainty of the FSR is effectively reduced by the large lever arm from the high number of modes generated by the low-finesse FPI. Thus, the absolute length of the spacer is measured at one wavelength, and the remaining uncertainty of all other peaks is reduced to the uncertainty in the variation in spacer length as a function of wavelength. This uncertainty, however, can be very substantial for wavelength ranges far away from the locked mode. A potential solution for astronomical purpose is to calibrate the FPI spectrum using an LFC in a laboratory. This would define the length of the spacer at every wavelength because the frequency of every peak can be measured and m is known (although the accuracy of this calibration will be much lower than the one reached in the locked mode). This information can be used to determine the position of *all* peaks from tracking one transmission by a locking scheme. Ideally, this strategy would allow absolute calibration using all transmission peaks of the FPI with an uncertainty limited by the ability to cross-reference the FPI spectrum to an external calibrator. This could be a cost-efficient way to apply the absolute wavelength accuracy of an LFC to astronomical spectrographs.

An externally tracked FPI can provide a light source for frequency calibration that allows cm s^{-1} precision measurements in astronomical Doppler experiments. For high-precision Doppler measurements, the externally tracked FPI is a huge improvement over traditional techniques like HCL calibration. The total cost of such a system can be estimated to be much lower than 20% of the typical cost for an astronomical LFC. The FPI calibrator is a high-precision calibration source that can become affordable for a wide range of observatories. All technology is available so that the proposed strategy is particularly interesting for upcoming experiments, such as CARMENES (Quirrenbach et al. 2012), HZPF (Mahadevan et al. 2012), and SPIRou (Artigau et al. 2011).

Acknowledgements. We thank Stuart Barnes for spotting an error in an earlier version of Fig. 1, and we thank the anonymous referee for a very helpful report. This research was supported by the European Research Council under the FP7 Starting Grant agreement number 279347. A.R. acknowledges research funding from DFG grant RE 1664/9-1.

References

Affolderbach, C., Mileti, G., Slavov, D., Andreeva, C., & Cartaleva, S. 2004, in Proc. of the 18th European Frequency and Time Forum (EFTF), The Institution of Electrical Engineers, London, paper 084, 409
Anderson, D. Z. 1984, Appl. Opt., 23, 2944
Arnold, A. S., Wilson, J. S., & Boshier, M. G. 1998, Rev. Sci. Instrum., 69, 1236
Artigau, É., Donati, J.-F., & Delfosse, X. 2011, in 16th Cambridge Workshop on Cool Stars, Stellar Systems, and the Sun, eds. C. Johns-Krull, M. K. Browning, & A. A. West, ASP Conf. Ser., 448, 771
Bennett, J. 1964, J. Opt. Soc. Am., 54, 612
Bjorklund, G. C. 1980, Opt. Lett., 5, 15
Black, E. D. 2001, Am. J. Phys., 69, 79
Born, M., & Wolf, E. 1999, Principles of Optics (Cambridge: Cambridge University Press)
Braje, D. A., Kirchner, M. S., Osterman, S., Fortier, T., & Diddams, S. A. 2008, Eur. Phys. J. D, 48, 57
Brault, J. W. 1987, Mikrochimica Acta, 3, 215
de Denus-Baillargeon, M. M., T., S., Larouche, S., & Martinu, L. 2014, Appl. Opt., 53, 2616
Drever, R. W. P., Hall, J. L., Kowalski, F. V., et al. 1983, Appl. Phys. B: Lasers Opt., 31, 97
Ennos, A. E. 1966, Appl. Opt., 5, 51
Fox, R. W., Oates, C. W., & Hollberg, L. W. 2003, Cavity-Enhanced Spectroscopies. Series: Experimental Methods in the Physical Sciences (Elsevier), 40, 1
Halverson, S., Mahadevan, S., Ramsey, L., et al. 2012, SPIE 8446, Ground-based and Airborne Instrumentation for Astronomy IV, 84468 [arXiv:1209.2704]
Henry, C. H. 1986, J. Lightwave Technol., 4, 298
Kerber, F., Nave, G., Sansonetti, C. J., Bristow, P., & Rosa, M. R. 2007, in The Future of Photometric, Spectrophotometric and Polarimetric Standardization, ed. C. Sterken, ASP Conf. Ser., 364, 461
Lichten, W. 1985, J. Opt. Soc. Am. A, 2, 1869
Lichten, W. 1986, J. Opt. Soc. Am. A, 3, 909
Mahadevan, S., Ramsey, L., Bender, C., et al. 2012, in SPIE Conf. Ser., 8446
Maiolino, R., Haehnelt, M., Murphy, M. T., et al. 2013 [arXiv:1310.3163]
Marcy, G. W., & Butler, R. P. 1992, PASP, 104, 270
Marcy, G. W., & Butler, R. P. 1998, ARA&A, 36, 57
Mayor, M., & Udry, S. 2008, Phys. Scr., 130, 4010
Meissner, K. 1941, J. Opt. Soc. Am., 31, 405
Mroziewicz, B. 2008, Opto-Electron. Rev., 16, 347
Murphy, M. T., Udem, T., Holzwarth, R., et al. 2007, MNRAS, 380, 839
Neuhaus, R. 2009, Diode laser locking and linewidth narrowing, Retrieved online from http://www.toptica.com
Osinski, M., & Buus, J. 1987, IEEE J. Quantum Electron., 23, 9
Osterbrock, D. E., Fulbright, J. P., Martel, A. R., et al. 1996, PASP, 108, 277
Pepe, F., & Lovis, C. 2008, in 2007 ESO Instrument Calibration Workshop, eds. A. Kaufer, & F. Kerber (Heidelberg Berlin: Springer Verlag), 375
Phillips, D. F., Glenday, A. G., Li, C.-H., et al. 2012, Opt. Exp., 20, 13711
Quinlan, F., Ycas, G., Osterman, S., & Diddams, S. A. 2010, Rev. Sci. Instrum., 81, 3105
Quirrenbach, A., Amado, P. J., Seifert, W., et al. 2012, in SPIE Conf. Ser., 8446
Redman, S. L., Ycas, G. G., Terrien, R., et al. 2012, Astrophys. J., Suppl. Ser., 199, 2
Ricci, L., Weidemüller, M., Esslinger, T., et al. 1995, Opt. Commun., 117, 541
Riehle, F. 1998, Meas. Sci. Technol., 9, 1042
Saliba, S. D., Junker, M., Turner, L. D., & Scholten, R. E. 2009, Appl. Opt., 48, 6692
Schäfer, S., & Reiners, A. 2012, in SPIE Conf. Ser., 8446
Schmidt, P. O., Kimeswenger, S., & Käufl, H. U. 2008, in 2007 ESO Instrument Calibration Workshop, ed. A. Kaufer, & F. Kerber, 409
Stanley, R., & Andrew, K. 1964, J. Opt. Soc. Am., 54, 625
Steck, D. A. 2010, available online at http://steck.us/alkalidata
Steinmetz, T., Wilken, T., Araujo-Hauck, C., et al. 2008, Science, 321, 1335
Steinmetz, T., Wilken, T., Araujo-Hauck, C., et al. 2009, Appl. Phys. B: Lasers Opt., 96, 251
Struve, O. 1952, The Observatory, 72, 199
Szipöcs, R., Ferencz, K., Spielmann, C., & Krausz, F. 1994, Opt. Lett., 19, 201
Udem, T., Holzwarth, R., & Hänsch, T. W. 2002, Nature, 416, 233
Vanier, J., & Mandache, C. 2007, Appl. Phys. B: Lasers Opt., 87, 565
Wildi, F., Pepe, F., Lovis, C., et al. 2009, in SPIE Conf. Ser., 7440
Wildi, F., Pepe, F., Chazelas, B., Lo Curto, G., & Lovis, C. 2010, in SPIE Conf. Ser., 7735
Wilken, T., Lovis, C., Manescau, A., et al. 2010, MNRAS, 405, L16
Ye, J., Swartz, S., Jungner, P., & Hall, J. L. 1996, Opt. Lett., 21, 1280